Steam reforming of toluene and naphthalene as tar surrogate in a gliding arc discharge reactor

Hao Zhang[a], Fengsen Zhu[a, b, c], Xiaodong Li[a,*], Ruiyang Xu[a], Li Li[a], Jianhua Yan[a], Xin Tu[c,*]

[a] *State Key Laboratory of Clean Energy Utilization, Zhejiang University, Hangzhou 310027, China*

[b] *Zhejiang Electric Power Design Institute Co. Ltd, Hangzhou 310012, China*

[c] *Department of Electrical Engineering and Electronics, University of Liverpool, Liverpool L69 3GJ, UK*

Abstract:

Steam reforming of mixed toluene and naphthalene as tar surrogate has been investigated in an AC gliding arc discharge plasma, with particular emphasis on better understanding the effect of steam and CO_2 on the reaction performance. Results show that H_2, C_2H_2 and CO are the major gas products in the plasma steam reforming of tar for energy recovery. The addition of a small amount of steam remarkably enhances the conversions of both toluene and naphthalene, from 60.4% to 76.1% and 57.6% to 67.4%, respectively, as ·OH radicals formed by water dissociation create more reaction pathways for the conversion of toluene, naphthalene and their fragments. However, introducing CO_2 to this process has a negative effect on the tar reforming. Optical emission spectroscopic diagnostics has shown the formation of a variety of reactive species in the plasma process. Trace amounts of monocyclic and bicyclic aromatic condensable by-products are also detected. The destruction of toluene and naphthalene can be initiated through the collisions of tar surrogates with energetic electrons, N_2 excited species, ·OH and O radicals etc. Further optimization of the plasma tar destruction is still needed because the complexity of the tar component in a practical gasifier could decrease the tar conversions.

Keywords: gliding arc discharge; tar surrogate; toluene; naphthalene; steam reforming

1. Introduction

Increasing depletion of fossil fuels and growing concerns about environmental issues (e.g., global

*Corresponding authors.

Email addresses: lixd@zju.edu.cn (X. Li), xin.tu@liv.ac.uk (X. Tu)

warming and disposal of waste) as well as the growing demand for clean fuels and chemical feedstocks has motivated the utilization of biomass and municipal solid waste (MSW) in the past two decades [1, 2]. Among various thermochemical conversion processes, gasification has attracted particular interest because it provides a flexible and efficient way for converting biomass or MSW to valuable syngas, which can be used in gas turbine or engine but also used as valuable chemical feedstocks for the synthesis of platform chemicals and liquid fuels [3-6]. However, the contamination of syngas with impurities, such as particulate matters, alkali metal salts, acid gases and tars cannot be avoided in the gasification and requires downstream gas cleaning [5]. Among these, tar is the most harmful byproduct, as upon cooling and condensing, problems of fouling, clogging and corrosion can be caused in downstream equipment and pipelines [7-9], resulting in high operational costs and even plant shut-down. Therefore, effective removal of tar has been regarded as a key challenge limiting the commercialization of gasification technologies [10]. Tar is a complex mixture of condensable aromatics compounds, such as benzene, toluene, naphthalene, with general content of 1 ~ 100 g/m^3, depending on the feedstock and gasifier type [1, 3, 11]. It should be noted that the permissible tar content in syngas is only around 100 mg/m^3 for reciprocating internal combustion engines and even lower for syngas end-use applications, e.g., gas turbines and chemical synthesis [1, 5].

Various techniques have been proposed for the removal or destruction of tar after a gasifier, including mechanical separation, thermal cracking and catalytic cracking or reforming [12]. Mechanical separation method can cause secondary pollution and waste chemical energy associated with tars [6]. Thermal cracking requires very high temperature (normally >1000 ^{o}C), incurring considerably high energy consumption [13]. Although catalytic reforming can lower the reaction temperatures to around 600 ^{o}C, rapid deactivation of the catalysts by sintering, poisoning and fouling severely limits its practical application [6].

In the last decade, non-thermal plasma technology is increasingly considered as an attractive alternative, because it enables the thermodynamically unfavorable destruction of tar to occur with a reduced energy cost under mild conditions (i.e., lower temperature and atmospheric pressure). In non-thermal plasmas, the electrical energy is selectively applied to generating highly energetic electrons (normally 1-10 eV), which is high enough to directly activate the reactants and produce highly reactive species (i.e., radicals, excited atoms, molecules and ions) for the effective initiation and propagation of chemical reactions [1, 14, 15]. Simultaneously, the plasma gas temperature can remain at a

considerably low level (even room temperature), allowing for a high energy efficiency due to the limited heat loss [14]. Moreover, non-thermal plasma features merits of high reaction rate, fast attainment of steady state, instantaneous "on-and-off" and high specific productivity (compactness) [14]. In view of these unique advantages, non-thermal plasma provides high flexibility to utilize electricity from intermittent renewable sources, e.g., solar and wind, and offers a solution to the imbalance between energy production and consumption by renewable sources [16].

For this purpose, dielectric barrier discharge (DBD) [6, 7, 17], corona discharge [11], microwave discharge [5, 8], and gliding arc discharge (GAD) [1, 4, 18, 19] have been investigated for tar destruction. However, DBD and corona discharge suffer from relatively low energy density and/or heterogeneous distribution of reactive species, resulting in a limited processing capacity. For example, a DBD plasma can obtain up to 85-96% toluene conversion in the steam reforming process, but has a gas flow rate of only 100 ml/min [7]. Microwave discharge has a relatively high energy density, but the extra energy requirement for vacuum device restricts its practical applications [20].

Atmospheric pressure gliding arc discharge, has been considered as a promising route for tar destruction. It is a powerful transitional plasma that exhibits simultaneously a relatively high energy density, high electron temperature and density, as well as good nonequilibrium characteristics with low energy cost, providing high flexibility to work in a wide range of flow rates (processing capacity) and plasma power levels (up to several kW) [21, 22]. Toluene is the most commonly studied model tar compound because of its high thermal stability, simple structure and low boiling point [1, 3, 4, 6, 17, 23]. Naphthalene is also frequently investigated because it is another representative component of biomass/MSW tars [8, 11, 18].

Most of previous efforts in this field focused on the effect of different operating parameters on the conversion of individual tar surrogate. However, tar is a mixture of condensable hydrocarbons including PAHs and thus understanding the plasma processing of mixed tar surrogates is of critical importance. In addition, H_2O and CO_2 are often present in the producer gas from gasification, while the role of H_2O and CO_2 in the plasma destruction of tar has barely been reported and is still not clear [4]. In previous studies of individual tar compound destruction process by non-thermal plasmas, a toluene or naphthalene conversion of up to 95% can be achieved but with a low energy efficiency [18, 23]. Obviously, to advance the practical application of this promising technology, in-depth parametric studies under conditions that are closer to the practical situation, together with the identification of

products (both gaseous and liquid) and intermediate species are essential for the optimization of the process and gaining a better understanding of the mechanisms.

In this work, steam reforming of toluene (C_7H_8) and naphthalene ($C_{10}H_8$) as tar surrogate was investigated in an AC GAD plasma, with particular effort to understand the effect of steam and CO_2 on the plasma processing of mixed tar surrogates. The effects of tar concentration, steam and CO_2 addition, and preheating temperature on the tar reforming performance have been emphasized. The intermediate species, gaseous and liquid products were identified by optical emission spectroscopy (OES), gas chromatography (GC) and GC - mass spectrometer (GC-MS), respectively, which enabled us to get insights in the possible reaction mechanisms of the tar reforming process in GAD plasma.

2. Experimental

2.1 Experimental setup

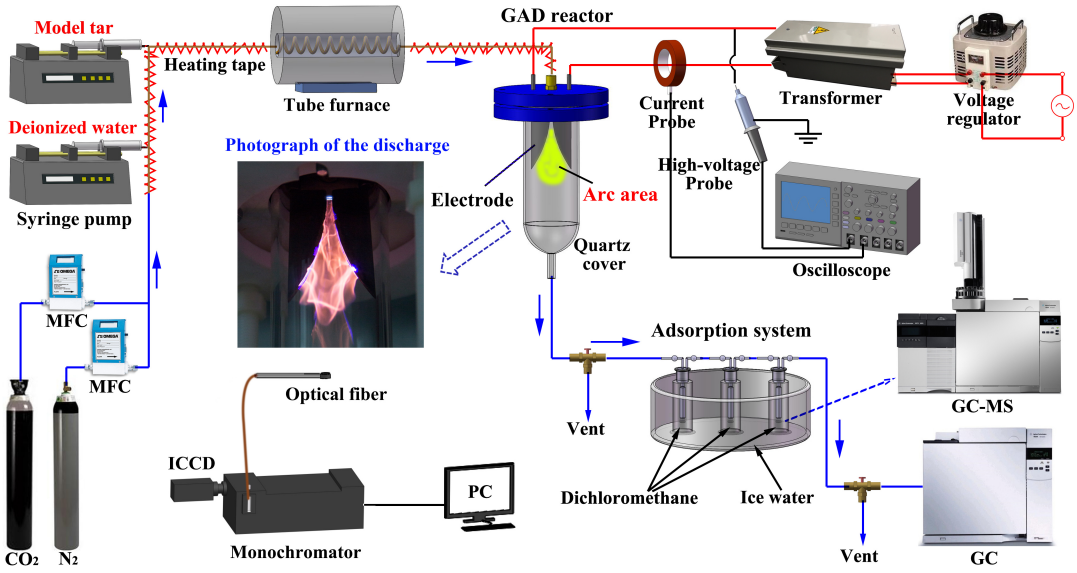

Fig. 1 Schematic diagram of the GAD assisted tar reforming experimental setup

The experimental setup of the GAD assisted tar reforming system is schematically shown in Fig. 1. The GAD reactor is composed of two divergent knife-shaped electrodes (stainless steel), which are fixed in an insulating bracket and placed symmetrically on both sides of a gas injector nozzle (with inner diameter of 1.5 mm). An AC 220V/15kV (transformer) equipped with a voltage regulator was connected to the electrodes. The discharge arc is initiated at narrowest gap point (2 mm) between the electrodes and is then pushed downstream along the electrodes by the gas flow until it extinguishes

due to the increased heat loss with increasing arc length. The formed plasma volume is exhibited in Fig. 1. The electrical signals of the discharge were measured using an oscilloscope (Tektronix DPO4034B) with a high-voltage probe (Tektronix P6015A) and a current probe (Tektronix TCP303).

N_2 was used as the carrier gas, because it is abundant in the air and has been proved to significantly facilitate the plasma reaction due to the formation of a variety of reactive species (e.g., $N_2(A)$ and $N_2(a')$) [22]. The feed N_2 and CO_2 from gas cylinders were controlled by mass flow controllers (MFC, Sevenstar D07). The tar (mixture of toluene and naphthalene) and water were injected into the gas tube by high-resolution syringe pumps (Harvard, 11 plus). The mixed stream with feed gases was then heated to 400 ^oC in a customized tube furnace (Hangzhou Lantu Instrument), to generate a steady-state vapor before flowing into the GAD reactor (for Section 3.3, the preheating temperature varied in range of 300-700 ^oC). To prevent condensation of the stream, a heating tape system (200 ^oC) was equipped in the gas line before and after the tube furnace. Three successive adsorption bottles: the first two containing hexane and the third empty, were placed in an iced water bath and at the exit of the GAD reactor to collect the condensable products in the effluent. Each experiment was performed three times with similar results and representative data are given. The studied conditions are tabulated in Table 1.

Table 1 The experimental conditions

Parameters	Input power (W)	Gas flow rate (L/min)	Tar concentration (g/m^3)*	C_7H_8 /$C_{10}H_8$ molar ratio	Preheating temperature (°C)	Steam content (%)	CO_2 content (%)
Values	350	4	2-22	10:1	300-700	0-20	0-30

The gaseous products were quantitatively measured by GC (Agilent 490 Micro GC) using a thermal conductivity detector (TCD) connected to Molsieve 5 A and Pora-PLOT U columns. The column temperature was set as 80 ^oC. The collected liquid samples were analyzed by GC-MS (Agilent 6890N GC/5975B MSD) equipped with a HP5 capillary column. The programming temperature was: 1) initial oven temperature of 40 ^oC holding for 2 min; 2) increases to 100 ^oC at a rate of 6 ^oC/min; 3) increases to 180 ^oC at a rate of 10 ^oC/min; 4) finally followed by an increase to 270 ^oC at a rate of 20 ^oC/min, holding for 5 min. The injection volume was 1 μL. The temperatures of the injector and detector were 280 ^oC and 250 ^oC, respectively. The electron-impact ionization of the mass spectrometer is 70 eV and the temperature of the ion source is 250 ^oC. The external standard method was used for the quantification of toluene and naphthalene. The calibration curves of toluene (R^2=0.9941) and

naphthalene (R^2=0.9932) were made from 5 standard solutions of toluene in hexane ranging from 500 to 3000 mg/L and naphthalene in hexane ranging from 50 to 500 mg/L, respectively. A 750-mm monochromator (PI-Acton 2750, grating: 2400 or 600 grooves/mm) equipped with an intensified charge-coupled device (ICCD, PI-MAX2, 512×512 pixel) was used to record the emission spectra of the plasmas. In the experiments, an optical fiber was placed at the exit of the reactor to collect the plasma emission.

2.2 Assessment methods

For the tar reforming process, the conversion of tar (toluene or naphthalene) was defined as follows:

$$X(\%) = \frac{\text{moles of tar converted}}{\text{moles of tar input}} \times 100\% \quad (1)$$

The yields of gaseous products (H_2, CO, CO_2, and C_xH_y) were calculated as follows:

$$Y_{H_2}(\%) = \frac{\text{moles of } H_2 \text{ produced}}{4\times(\text{moles of tar input}) + \text{moles of } H_2O \text{ input}} \times 100\% \quad (2)$$

$$Y_{CO}(\%) = \frac{\text{moles of CO produced}}{7\times(\text{moles of toluene input}) + 10\times(\text{moles of naphthalene input}) + \text{moles of } CO_2 \text{ input}} \times 100\% \quad (3)$$

$$Y_{CO_2}(\%) = \frac{\text{moles of } CO_2 \text{ produced}}{7\times(\text{moles of toluene input}) + 10\times(\text{moles of naphthalene input})} \times 100\% \quad (4)$$

$$Y_{C_xH_y}(\%) = \frac{X\times\text{moles of } C_xH_y \text{ produced}}{7\times(\text{moles of toluene input}) + 10\times(\text{moles of naphthalene input})} \times 100\% \quad (5)$$

In line with previous studies [1, 6, 17], the energy efficiency of the plasma reaction is defined as the grams of tar converted per kWh electricity:

$$\eta(\text{g/kWh}) = \frac{\text{grams of tar converted per min}}{\text{Discharge power (W)} \times 60/360000} \quad (6)$$

3. Results and discussions

3.1 Effect of steam concentration

The effect of steam concentration on the tar conversion and energy efficiency is illustrated in Fig. 2. Clearly, the addition of 4% steam remarkably enhances the conversions of both toluene and

naphthalene from 60.4% to 76.1% and 57.6% to 67.4%, respectively. However, a saturation or slight drop of tar conversion can be observed when introducing more steam (> 4%) into the plasma reaction. Similar results have been reported in previous works such as toluene steam reforming using a gliding arc discharge [1] and toluene oxidation in DBD [24] and corona discharge [25]. The addition of steam into the N_2 plasma forms ·OH radicals (see the spectra in Fig. 10) via water dissociation by electrons (R1) and N_2 excited species (R2) [1, 26]. The generated ·OH radicals are highly active in the destruction of toluene and naphthalene (e.g., R3-R5) and thus contribute to the enhanced tar conversion [1, 11, 27, 28].

$$H_2O + e \rightarrow H\cdot + \cdot OH + e \quad \text{R1}$$

$$H_2O + N_2^* \rightarrow H\cdot + \cdot OH + N_2 \quad \text{R2}$$

$$C_6H_5CH_3 + \cdot OH \rightarrow C_6H_5CH_2\cdot + H_2O \quad \text{R3}$$

$$C_6H_5CH_3 + \cdot OH + N_2 \rightarrow C_6H_5(OH)CH_3 + N_2 \quad \text{R4}$$

$$C_{10}H_8 + \cdot OH \rightarrow C_{10}H_7\cdot + H_2O \quad \text{R5}$$

Where N_2^* represents the N_2 excited species such as $N_2(A)$ and $N_2(X, v)$.

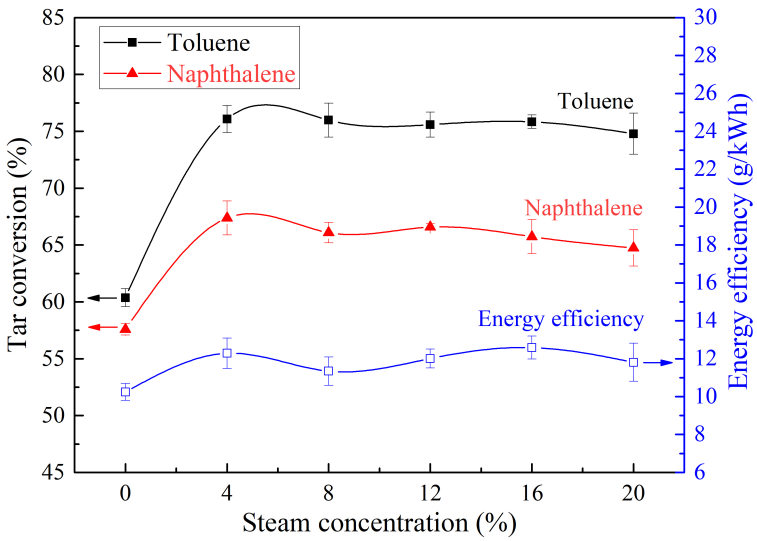

Fig. 2 Effect of steam concentration on tar conversion and energy efficiency

(Tar concentration 10 g/Nm^3, Preheating temperature 400 ^{o}C, Without CO_2 addition)

However, H_2O also has an adverse effect on the conversion of tar surrogate due to its electronegative characteristics. Both energetic electrons and N_2 excited species (e.g., $N_2(A)$ and $N_2(a')$)

present in the plasma contribute to the destruction of toluene and naphthalene via R6-R15 [25, 27]. Further increasing the steam concentration decreases the electron density and also quenches the formation of N_2^* species (especially $N_2(A)$, as evidenced in our previous study [26]), consequently limiting the conversion of toluene and naphthalene. Ye et al. have confirmed the suppressing effect of water on the population of N_2 excited species in the DBD decomposition of toluene using OES [29]. As shown in Fig. 2, the energy efficiency shows a similar variation tendency (10.2-12.6 g/kWh) as tar conversion.

$$C_6H_5CH_3 + e \rightarrow C_6H_5CH_2\cdot + H\cdot + e \quad \text{R6}$$

$$C_6H_5CH_3 + e \rightarrow C_6H_5\cdot + CH_3\cdot + e \quad \text{R7}$$

$$C_{10}H_8 + e \rightarrow C_{10}H_7\cdot + H\cdot + e \quad \text{R8}$$

$$C_{10}H_8 + e \rightarrow C_9H_7\cdot + CH\cdot + e \quad \text{R9}$$

$$C_6H_5CH_3 + N_2(A) \rightarrow C_6H_5CH_2\cdot + H\cdot + N_2 \quad \text{R10}$$

$$C_6H_5CH_3 + N_2(A) \rightarrow C_6H_5\cdot + CH_3\cdot + N_2 \quad \text{R11}$$

$$C_6H_5CH_3 + N_2(A) \rightarrow \cdot C_6H_4CH_3 + H\cdot + N_2 \quad \text{R12}$$

$$C_6H_5CH_3 + N_2(a'^1) \rightarrow C_5H_6 + C_2H_2 + N_2 \quad \text{R13}$$

$$C_{10}H_8 + N_2(A) \rightarrow C_{10}H_7\cdot + H\cdot + N_2 \quad \text{R14}$$

$$C_{10}H_8 + N_2(A) \rightarrow C_9H_7\cdot + CH\cdot + N_2 \quad \text{R15}$$

As clearly shown in Fig. 2 (also in the following sections), the conversion of toluene is 9-13% higher than that of naphthalene, indicating that toluene is more easy to be decomposed compared to naphthalene. Nunnally et al. also reported similar results in the plasma oxidative steam reforming of toluene and naphthalene using a gliding arc [4]. This phenomenon could be related to the inherent molecular structure and stability of these molecules. The H-abstraction reaction for tar destruction is more active in toluene due to the presence of methyl group in toluene [1]. In traditional thermal conversion processes, the kinetic reactivity of different tar molecules followed the order of toluene >> naphthalene > benzene [30].

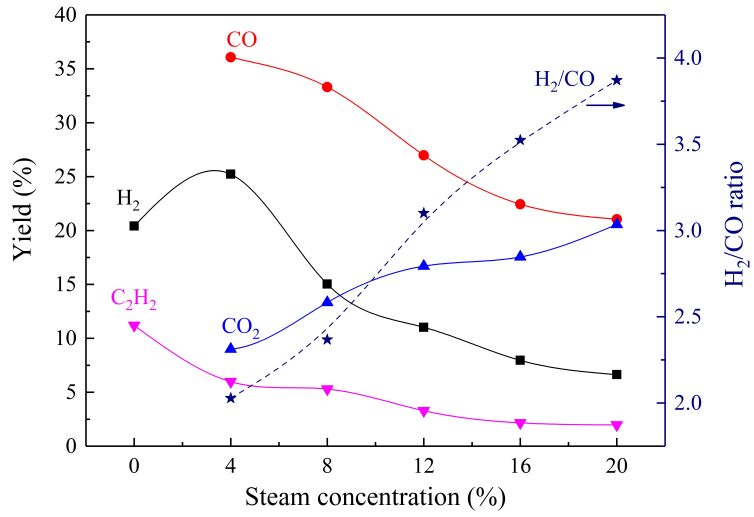

(a) Major gaseous products

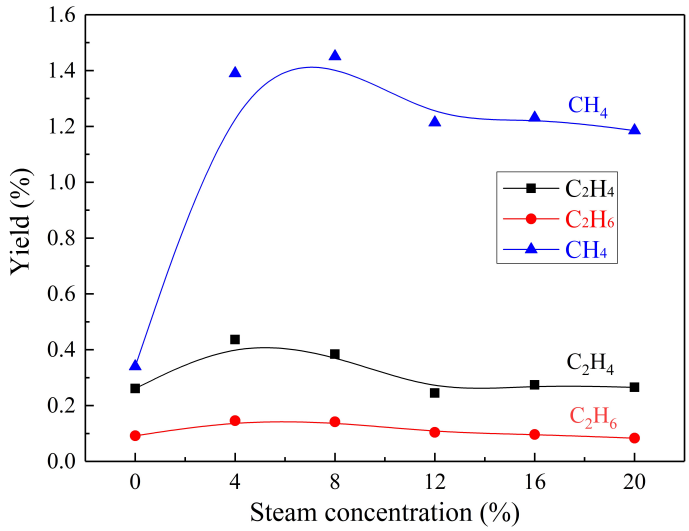

(b) Minor gaseous products

Fig. 3 Effect of steam concentration on (a) the yields of major gaseous products and H_2/CO ratio, and (b) the yields of minor gaseous products

(Tar concentration 10 g/Nm^3, Preheating temperature 400 ^{o}C, Without CO_2 addition)

The yields of major and minor gaseous products, together with H_2/CO ratio with rising tar concentration are given in Fig. 3. Similar to toluene decomposition using a rotating gliding arc [23], H_2 and C_2H_2 are identified as the two major H-containing gaseous products with yields of 6.6-25.2% and 2.0-11.2%, respectively. Clearly, the presence of steam in the system results in the formation of CO and CO_2 with even higher yields (21.1-36.1%, and 9.0-20.6%), due to the steam reforming of tar. CO has a higher yield than CO_2, because of the partial oxidation of tar model compounds and their

fragments in the plasma process. In a gliding arc system for steam reforming of toluene by Liu et al. [1], in addition to the generation of H_2, C_2H_2, CO and CO_2, C_2H_4 was also detected as a major gaseous product with a similar yield of CO. By contrast, the yield of C_2H_4 was less than 0.5% in this work, as shown in Fig. 3(b). The formation of these fuel gases with significant yields suggest that upgrading of the producer gas can be realized in the gliding arc plasma by converting the problematic tar into value-added products.

Clearly, the yields of gaseous products are strongly dependent on the steam concentration. The drop of CO yield and the augment of both CO_2 yield and H_2/CO with increasing steam addition are closely related to the water gas shift reaction (R16) in the plasma process, which reduces the CO formation but increases the formation of CO_2 and H_2. It should be noted that, the H_2 fraction in the gas effluent is increased but the H_2 yield drops (see Fig. 3(a)), because the increasingly injected H_2O was also considered as the H source in the calculation of H_2 yield. In line with other works [1, 31], the formation of C_2H_2 is suppressed when increasing the steam concentration, which can be attributed to the decreased probabilities of the ring cleavage of the tar molecules due to the decreased number density of electrons and reactive species (see R6-R15).

$$CO + H_2O \rightarrow CO_2 + H_2 \qquad \text{R16}$$

It is also important to note that the addition of steam in the plasma tar reforming significantly reduced the formation of carbon deposition, which is crucial to maintain a long-term operation of the plasma process.

3.2 Effect of tar concentration

The effect of input tar concentration on the conversion of tar with steam addition is shown in Fig. 4. The steam concentration was maintained at 12% based on the results in Section 3.1 and the steam content in practical producer gas. As expected, increasing tar concentration from 2 to 22 g/Nm^3 leads to a continuous drop of the conversions of both toluene and naphthalene from 85.9% and 74.0% to 68.9% and 59.7%, respectively. This should be attributed to the decreased specific energy input (SEI) on the injected tar, because the discharge power remained relatively constant in the experiments. Similar results have been reported in the previous researches [1, 4-6, 18].

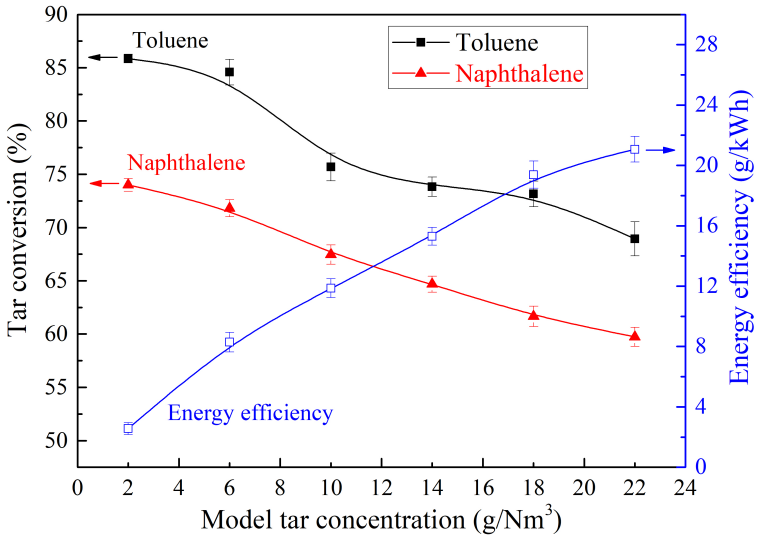

Fig. 4 Effect of tar concentration on tar conversion and energy efficiency

(Steam concentration 12%, Preheating temperature 400 ^{o}C, Without CO_2 addition)

Fig. 4 shows a trade-off between the tar conversion and energy efficiency. Increasing the tar concentration from 2 to 22 g/Nm^3 significantly decreases the conversion of tar but significantly enhances the energy efficiency from 2.6 to 21.1 g/kWh, which indicates more tar can be destructed although the conversion is decreased when increasing the tar concentration under a similar energy input level. Note that the energy efficiency for tar conversion obtained in this work is better than that for practical tar destruction using a microwave plasma (4.52 g/kWh) [32] and that for naphthalene destruction (3.6 g/kWh) using a GAD [33], but further enhancement of the performance is still needed to be economically competitive.

As exhibited in Fig. 5, although the conversions of tar decrease with increasing tar concentration, the yields of H_2 and C_2H_2 (and H_2/CO ratio) rise significantly, while the CO_2 yield drops remarkably, which is favorable for the upgrading of the producer gas due to the enhanced heating value of the producer gas. Similar results were reported in the destruction of anthracene using a GAD [34]. Obviously, the decrease of O/C ratio and the increase of H/O ratio in the plasma process leads to the drop of CO_2 yield and the increase of H_2/CO ratio, respectively.

Clearly, the tar concentration can influence significantly the performance of the plasma-assisted tar destruction process. If the plasma technology can be used in a practical gasifier, power and the flow rate of the carrier gas (N_2) need to be appropriately controlled to deal with the different concentration of tar.

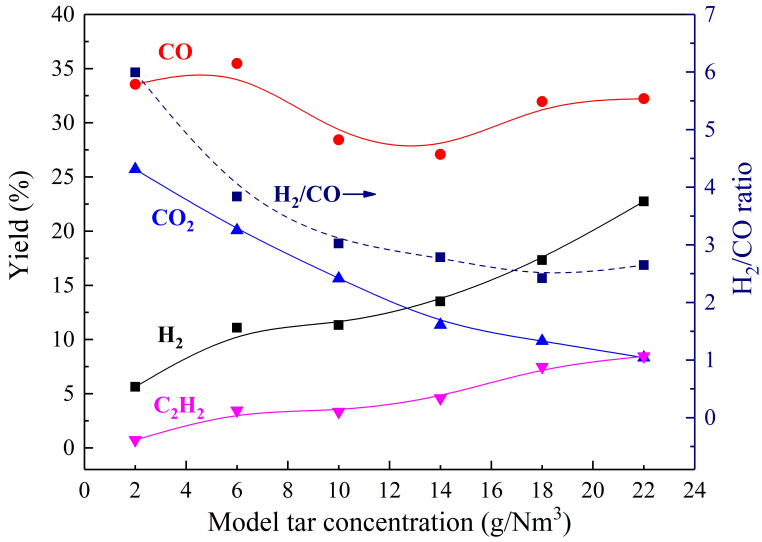

(a) Major gaseous products

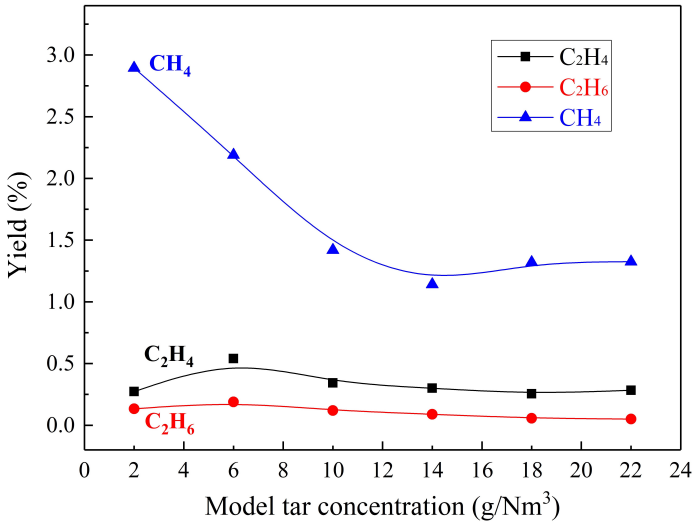

(b) Minor gaseous products

Fig. 5 Effect of tar concentration on (a) the yields of major gaseous products and H_2/CO ratio, and (b) the yields of minor gaseous products

(Steam concentration 12%, Preheating temperature 400 ^{o}C, Without CO_2 addition)

3.3 Effect of preheating temperature

In the experiments, the mixture of tar and carrier gas should be preheated to generate a steady-state vapor before going into the reactor. Therefore, it is crucial to understand the influence of the preheating temperature on the reaction performance. Fig. 6 shows that increasing the preheating temperature from 300 to 500 ^{o}C slightly enhances the conversions of toluene and naphthalene from 74.0% to 77.9% and 66.3% to 69.8%, respectively, due to the increased energy input into the reaction

system. However, a slight drop of the tar conversion is surprisingly followed when further rising the preheating temperature to 700 °C. This could be related to the increased feed flow speed (and thus decreased retention time of reactants in plasma) because of the increased temperature of the injected gas stream. Similar results have been observed in gliding arc assisted methanol decomposition processes [35]. Fig. 7 shows that with increasing preheating temperature, the yields of gaseous products follow similar variation profiles as that of the tar conversions, except for CO and C_2H_2 that show monotonic increases in the yields. This is probably related to the enhanced reaction between the superheated steam and some light hydrocarbon molecules.

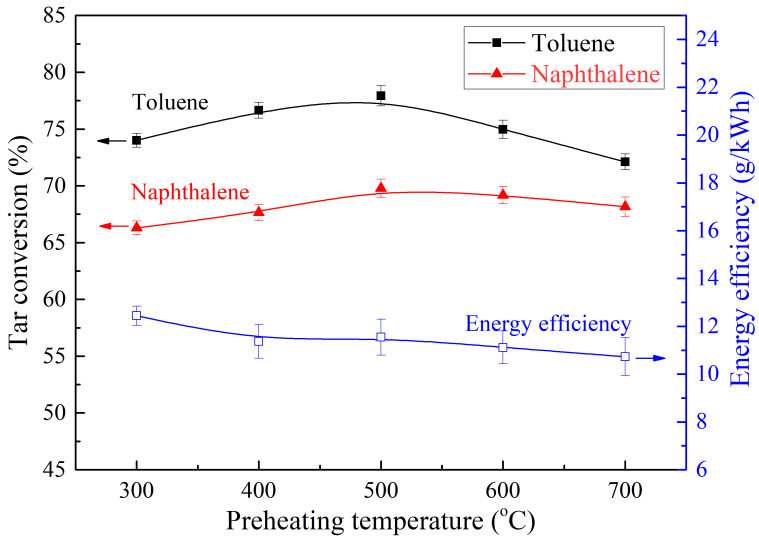

Fig. 6 Effect of preheating temperature on tar conversion and energy efficiency (Tar concentration 10 g/Nm^3, Steam concentration 12%, Without CO_2 addition)

Note previous works usually used a low preheating temperature (200-300 °C) [5, 7] which is much lower than that of the producer gas from a gasifier (e.g., 650-900 °C). This work has demonstrated that the GAD discharge can maintain stable at a higher temperature (700 °C), offering the flexibility to be used in a wider temperature window for practical applications.

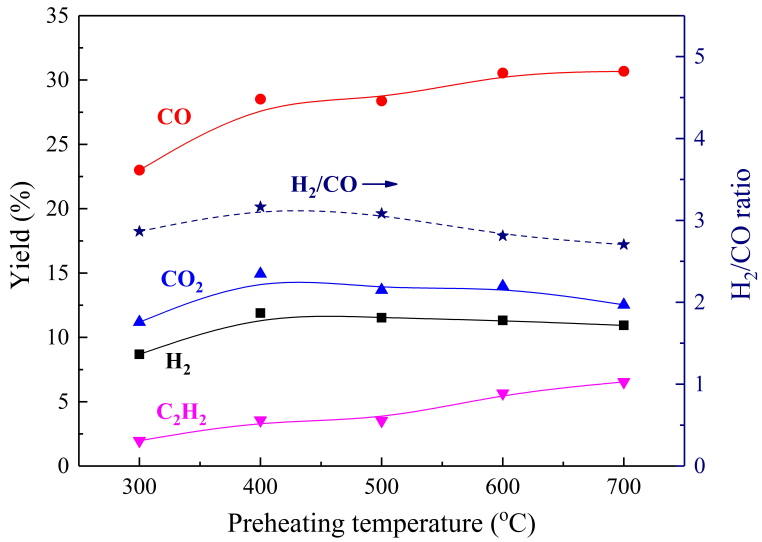

(a) Major gaseous products

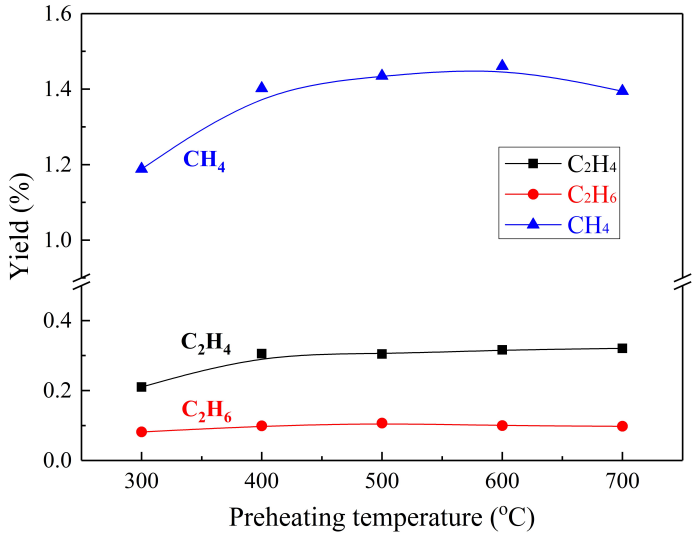

(b) Minor gaseous products

Fig. 7 Effect of preheating temperature on (a) the yields of major gaseous products and H_2/CO ratio, and (b) the yields of minor gaseous products

(Tar concentration 10 g/Nm^3, Steam concentration 12%, Without CO_2 addition)

3.4 Effect of CO_2 addition

Understanding the effect of CO_2 on the plasma destruction of tar surrogate is important as CO_2 is one of the major components of the producer gas from gasification (15-25%) [36]. Clearly, the addition of CO_2 is detrimental to the destruction of tar in the plasma process, as seen from Fig. 8. Both the conversions of toluene and naphthalene and the energy efficiency are decreased with increasing CO_2

concentration. A reasonable explanation for this is given below. The addition of CO_2 gives rise to the formation of O via the dissociation reaction, which can contribute to the destruction of toluene (e.g., R17) and naphthalene (e.g., R18). However, the reaction rate constant of R17 and R18 is typically 1-4 orders of magnitude lower than that of the reaction between N_2 excited species (e.g., $N_2(A)$) and tar molecules (e.g., R10 and R19). The N_2 concentration drops upon rising CO_2 concentration and simultaneously, the dissociation of CO_2 can deplete some of the N_2 excited species via the collision processes, which significantly reduces the population of N_2 excited species and thus decreases the tar conversion. In a simulation work of Valentin et al. [11], $N_2(A)$ has been demonstrated to be of vital importance to the destruction of naphthalene in plasma chemical processes. In addition, when CO_2 is added into the system, part of the input energy could be used for the decomposition of CO_2, thus decreasing the tar conversion. To reduce the negative effect of CO_2 on the tar destruction, more carrier gas (N_2) can be injected into the plasma system to enhance the formation of N_2^* reactive species. Moreover, the integration of gasification with carbon capture could also be a promising solution to tackle this challenge.

$C_6H_5CH_3 + O \rightarrow C_6H_5CH_2\cdot + \cdot OH \quad k=1.05\times10^{-12}$ cm^3/s (T=1150K-1350K) [37] R17

$C_{10}H_8 + O \rightarrow C_{10}H_7\cdot + \cdot OH \quad k=(3.19\text{-}181.8)\times10^{-15}$ cm^3/s (T=800K-1421K) [37] R18

$C_6H_5CH_3 + N_2(A) \rightarrow C_6H_5CH_2\cdot + H\cdot + N_2 \quad k=6.0\times10^{-11}$ cm^3/s [31] R10

$C_{10}H_8 + N_2(A) \rightarrow$ products $\quad k=1.6\times10^{-10}$ cm^3/s [11] R19

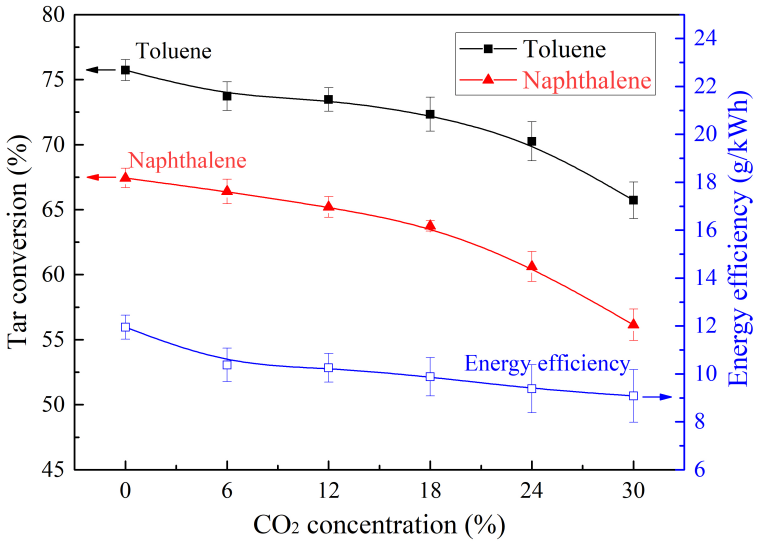

Fig. 8 Effect of CO_2 concentration on tar conversion and energy efficiency

(Tar concentration 10 g/Nm^3, Steam concentration 12%, Preheating temperature 400 ^{o}C)

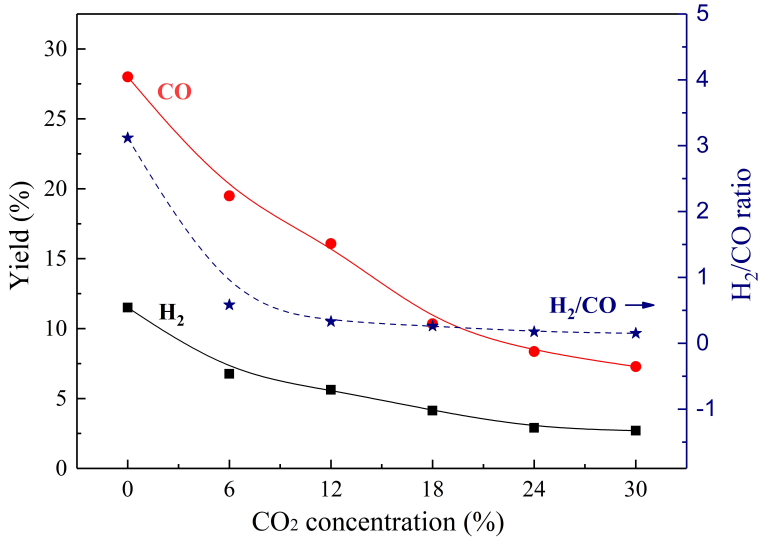

(a) Major gaseous products

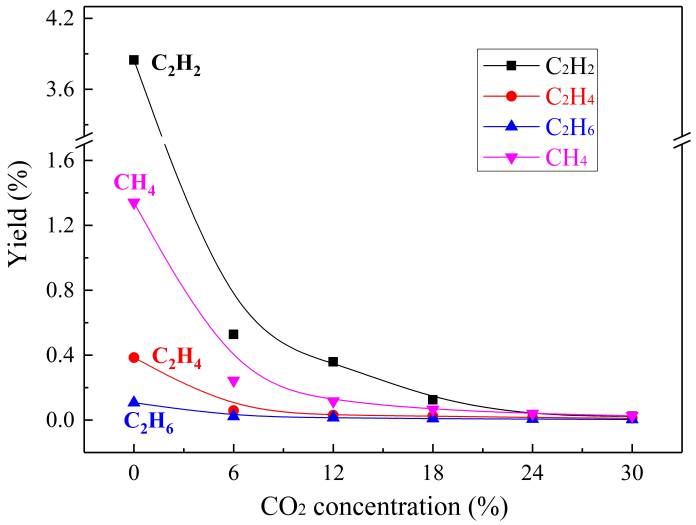

(b) Minor gaseous products

Fig. 9 Effect of CO_2 concentration on (a) the yields of major gaseous products and H_2/CO ratio, and (b) the yields of minor gaseous products

(Tar concentration 10 g/Nm^3, Steam concentration 12%, Preheating temperature 400 ^{o}C)

As exhibited in Fig. 9, the CO_2 concentration significantly influences the formation of gaseous products. The yields of H-containing gaseous products, i.e., H_2, C_2H_2, CH_4, C_2H_4 and C_2H_6, are all pronouncedly reduced upon the addition of CO_2. In the experiments, the fraction of CO in the effluent gas increases significantly with rising CO_2 concentration, but its yield decreases (see Fig. 9(a)), because the increasing amount of CO_2 introduced is considered in the calculation of CO yield. The rising amount of CO_2 depletes more H_2 molecules due to the reverse water gas shift reaction (R20),

resulting in a continuous drop in the H_2 yield. In addition, the H_2 yield is decreased due to the decreased number density of N_2 excited species which contribute to the formation of H_2 via the H-abstraction of tar molecules (as abovementioned, see R10, R12, R14). It is then expected that the H_2/CO ratio declines upon rising CO_2 concentration.

$$CO_2 + H_2 \rightarrow CO + H_2O \qquad \text{R20}$$

The suppression of CH_4, C_2H_2, C_2H_4 and C_2H_6 yields upon increasing CO_2 concentration should be attributed to the reduced chance of ring cleavage of tar molecules by N_2 excited species that can release small hydrocarbon gases.

The comparison of the results in Sections 3.1-3.4 allow us to conclude that the "best results" can be obtained at a tar concentration of 6-10 g/Nm^3, a steam concentration of 4-12%, a preheating temperature of 400 ^{o}C and a CO_2 concentration of 0-12%, yielding a toluene conversion of 75-85%, a naphthalene conversion of 65-72%, H_2 and CO yields of 6-25% and 16-36%, and an energy efficiency of 8-16 g/kWh.

3.5 Identification of intermediate species and liquid byproducts

Optical emission spectroscopy has been used to gain new insights into the formation of reactive species in the plasma chemical reactions under the studied conditions. Typical emission spectra (200-900 nm) of the plasma with N_2+tar, N_2/H_2O+tar and N_2/H_2O/CO_2+tar are illustrated in Fig. 10. Clearly, the N_2+tar spectra are dominated by strong CN ($B^2\Sigma \rightarrow X^2\Sigma$) violet bands with various vibrational transitions. The formation of CN is related to the reactions between N_2 (or N) and various C-containing species (such as CH_x ($x \leqslant 4$) and C_2) [22]. Weak C_2 ($d^3\Pi_g \rightarrow a^3\Pi_u$) bands in the range of 510-517 nm is also observed. The addition of steam into the system significantly changes the formation of intermediate species. Besides the CN and C_2 spectra, strong OH ($A^2\Sigma^+ \rightarrow X^2\Pi$) bands in 280-325 nm, noticeable NH ($A^3\Pi \rightarrow X^3\Sigma$) line at 336.0 nm, weak NO γ ($A^2\Sigma^+(v') \rightarrow X^2\Pi(v'')$) bands in 225-250 nm and weak Hα line at 656.3 nm are observed in the N_2/H_2O+tar spectra. Obviously, ·OH radical forms from the dissociation of H_2O molecules and can then contribute significantly to the destruction of tar molecules (as abovementioned). The N atoms that formed from electron impact dissociation of N_2, give rise to the formation of NH radical and NO radical via the reactions with H, H_2, H_2O or ·OH

and with ·OH, respectively [1, 26]. The existence of NH, NO and CN indicates the formation of NH_3, NO_x (nitrogen oxides) and HCN in the reaction (as previously reported in literature [38, 39]) which can be confirmed by the measurement using a Fourier Transform Infrared (FTIR) Spectrometer in this work (see Table S1 in Supplementary Data). As seen from Table S1, NO and HCN show the highest yields in $N_2/H_2O/CO_2$/tar and N_2/H_2O/tar respectively, which is in line with the OES results in Fig. 10, where strong bands of NO and CN were observed under corresponding conditions. Further addition of CO_2 into N_2/H_2O+tar gives rise to the occurrence of weak CO ($A^1\Pi \rightarrow X^1\Sigma$) bands and significantly decreases the intensity of CN spectral lines.

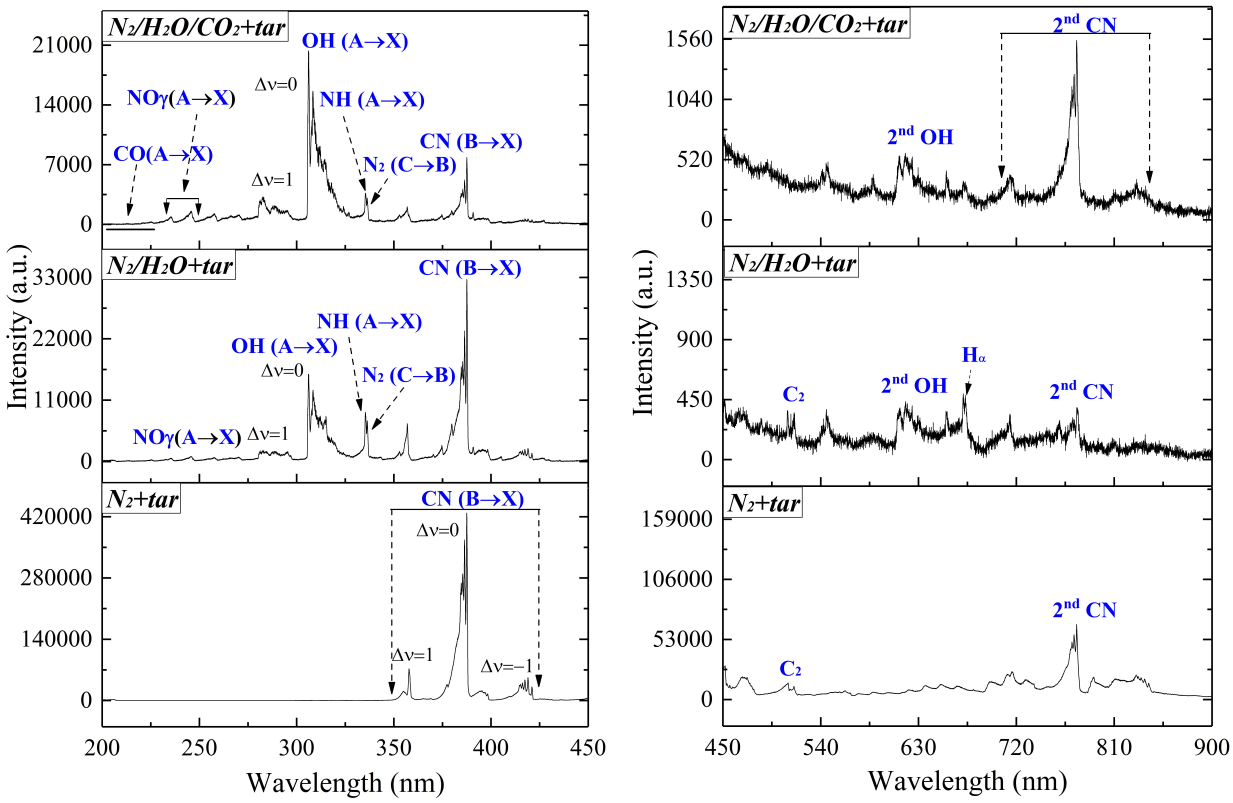

Fig. 10 Typical emission spectra of the plasmas with different mixtures. Tar concentration 10 g/Nm^3; H_2O concentration 12%; CO_2 concentration 12%. (slit width: 0.5 mm, exposure time: 0.20 s, gratings: 2400 g/mm (200-450 nm), 600 g/mm (450-900 nm))

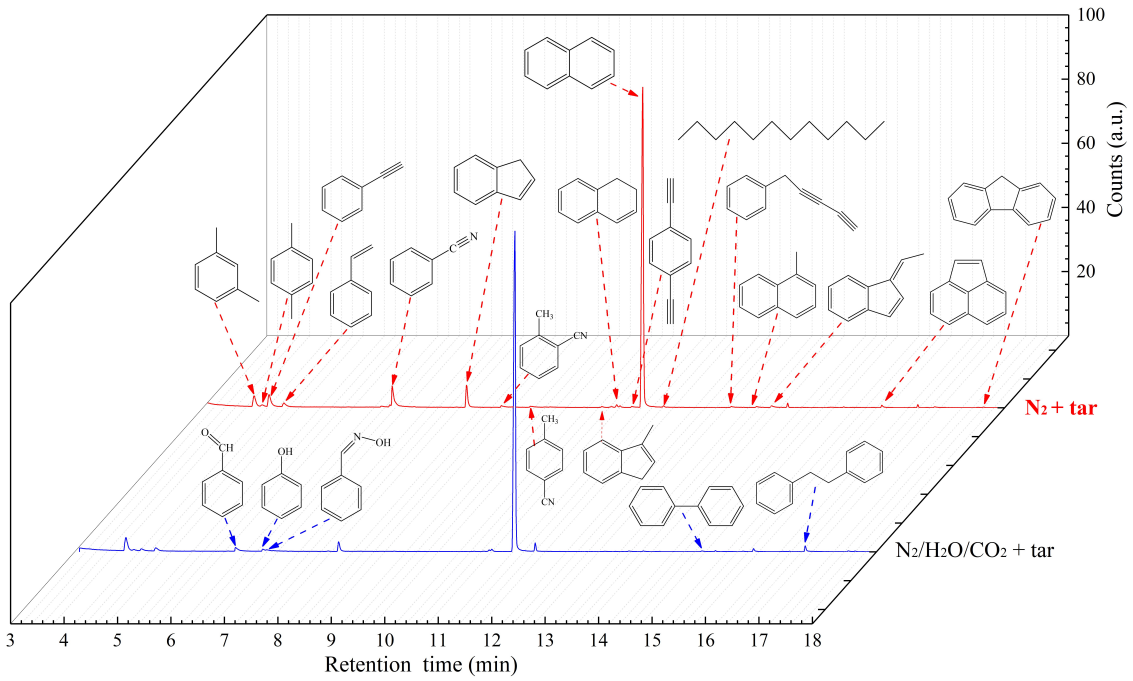

Fig. 11 GC-MS results of the liquid products under different conditions

(Tar concentration 10 g/Nm^3; H_2O concentration 12%; CO_2 concentration 12%. Toluene is not included.)

Table 2 Identified liquid byproducts by GC-MS (toluene is not included)

No.	Retention time (min)	N_2 + Tar	$N_2/H_2O/CO_2$ + Tar
1	3.960	**1,3-dimethylbenzene (C_8H_{10})***	**1,3-dimethylbenzene (C_8H_{10})**
2	4.108	*p*-Xylene (C_8H_{10})	*p*-Xylene (C_8H_{10})
3	4.239	**Phenylacetylene (C_8H_6)**	Phenylacetylene (C_8H_6)
4	4.512	Styrene (C_8H_8)	Styrene (C_8H_8)
5	6.013	--	**Benzaldehyde (C_7H_6O)**
6	6.524	---	**Phenol (C_6H_6O)**
7	6.541	**Benzonitrile (C_7H_5N)**	---
8	6.601	---	(Z)-Benzaldehyde oxime (C_7H_7NO)
9	7.936	**Indene (C_9H_8)**	**Indene (C_9H_8)**
10	8.601	1-isocyano-2-methylbenzene (C_8H_7N)	---
11	9.159	Benzonitrile (C_8H_7N)	---
12	10.465	3-methyl-1H-indene ($C_{10}H_{10}$)	---

13	10.821	1,2-dihydronaphthalene ($C_{10}H_{10}$)	1,2-dihydronaphthalene ($C_{10}H_{10}$)
14	11.070	1,4-diethynylbenzene ($C_{10}H_6$)	---
15	11.230	**Naphthalene ($C_{10}H_{12}$)**	**Naphthalene ($C_{10}H_{12}$)**
16	11.616	Dodecane ($C_{12}H_{26}$)	**Dodecane ($C_{12}H_{26}$)**
17	12.892	2,4-pentadiynylbenzene ($C_{11}H_8$)	---
18	13.373	1-methylnaphthalene ($C_{11}H_{10}$)	1-methylnaphthalene ($C_{11}H_{10}$)
19	13.640	1-ethylidene-1H-indene ($C_{11}H_{10}$)	1-ethylidene-1H-indene ($C_{11}H_{10}$)
20	15.700	Acenaphthylene ($C_{12}H_8$)	Acenaphthylene ($C_{12}H_8$)
21	16.697	Bibenzyl ($C_{14}H_{14}$)	**Bibenzyl ($C_{14}H_{14}$)**
22	17.504	Fluorene ($C_{13}H_{10}$)	Fluorene ($C_{13}H_{10}$)

*The major by-products are presented in bold in the table

GC-MS has been used to qualitatively analyze the liquid end-products, in order to further understand the reaction mechanisms. The GC-MS results under different conditions are illustrated in Fig. 11 and tabulated in Table 2. The GC-MS spectrum of N_2/H_2O+tar is similar with that of N_2/H_2O/CO_2+tar and is thus not exhibited. Clearly, a variety of liquid byproducts are detected, of which mostly are monocyclic and bicyclic aromatic compounds. No tricyclic or higher aromatic compounds are detected in the liquid sample, indicating that polymerization reaction is not active in this process. The major liquid by-products in the N_2+tar plasma are 1,3-dimethylbenzene (C_8H_{10}), phenylacetylene (C_8H_6), indene (C_9H_8) and the N-containing benzonitrile (C_7H_5N). As expected, the addition of H_2O or H_2O/CO_2 into N_2+tar give rises to the formation of several oxygenated aromatic compounds, such benzaldehyde (C_7H_6O), phenol (C_6H_6O) and (Z)-Benzaldehyde oxime (C_7H_7NO). As mentioned in Sections 3.1 and 3.4, the addition of H_2O or H_2O/CO_2 decreases the number density of energetic electrons and N_2 excited species that are active in the destruction of toluene and naphthalene, contributing to the reduced liquid by-products in N_2/H_2O/CO_2+tar (especially N-containing products, see Table 2 and Fig. 11). All the byproducts exhibit spectrum intensity of 1-3 orders of magnitude lower in comparison to the residue naphthalene (>65% naphthalene has been destructed), suggesting a relatively thorough treatment of the model tar compounds in this gliding arc plasma. Note that, in DBD plasmas [17], several liquid byproducts (e.g., benzene and ethylbenzene) were detected with high contents that were comparable to the model tar compounds, which is apparently unfavorable in the tar

destruction process.

In comparison to previous study of toluene steam reforming process in gliding arc [1], more bicyclic aromatic compounds (e.g., 1-methylnaphthalene ($C_{11}H_{10}$), acenaphthylene ($C_{12}H_8$), bibenzyl ($C_{14}H_{14}$), fluorene ($C_{13}H_{10}$)) are generated in this work due to the presence of naphthalene in the model tar compounds. In addition, in the toluene decomposition process in a N_2 gliding arc plasma, various branched alkanes compounds were detected [23]. However, in this work, only trace amount of dodecane is found in both the N_2+tar and $N_2/H_2O/CO_2$+tar spectra, resulting apparently from the cleavage of the toluene ring and the recombination and hydrogenation of the intermediate molecular fragments.

The destruction of toluene and naphthalene molecules can be initiated through the collisions with energetic electrons, N_2 excited species, ·OH (in the presence of H_2O) and O radicals (in the presence of CO_2 or H_2O, with minor role), as shown in R3-R5, R6-R15 and R17-R18, producing benzyl ($C_6H_5CH_2$·), phenyl (C_6H_5·), cyclopentadiene (C_5H_6), naphthyl ($C_{10}H_7$·) and indenyl (C_9H_7·), etc. The propagation of the subsequent reactions between various active intermediate species and monocyclic or bicyclic molecules and radicals results in the formation of the complex end-products.

Specifically, the combination of benzyl radicals with acetylene and propargyl radicals could form indene and 1,2-dihydronaphthalene, respectively. Benzyl radicals could also react with ·OH radicals to produce benzaldehyde in the presence of H_2O. By the combination with small intermediate species, such as ·OH and CN, phenyl radicals can convert into phenol and benzonitrile, respectively. In addition, the main monocyclic aromatic compounds exhibit a substitution with either a CN, or a two-carbon containing group, indicating an alkylation of benzene with either ethyne or ethene. The formed naphthyl radicals could react with methyl and acetylene radicals to produce 1-methylnaphthalene and acenaphthylene ($C_{12}H_8$). Indenyl radicals could form indene and 1-ethylidene-1H-indene ($C_{11}H_{10}$) via the reactions with H· and ethyl radicals, respectively. The direct hydrogenation reaction of naphthalene can also generate the identified 1,2-dihydronaphthalene ($C_{10}H_{10}$).

Previous studies showed that significantly high conversions of toluene or naphthalene can be obtained in non-thermal plasma assisted destruction of individual tar compound at similar tar concentrations with this work, e.g., a toluene conversion of 85-95% in DBD [7, 17] or GAD plasmas [23] and even 99% in microwave plasmas [5]; a naphthalene conversion of 79-95% in GAD plasmas [18, 19]. This work indicates that the coexistence of two tar compounds can probably decrease the

conversion of each tar compound in the plasma process, i.e., a toluene conversion of 60-85.8% and a naphthalene conversion of 56.1-74.0%. It is then expected that the tar conversions could be further lowered if the non-thermal plasma technology can be used in a practical gasifier, due to the complex components of tar. In addition, the presence of more tar compounds in the system remarkably increased the kinds of liquid compounds generated in the products, which is obviously harmful for the process. Therefore, further optimization of the plasma chemical process is still highly needed in terms of the reactor design, power source design and reaction conditions etc., to enable a more thorough treatment of the tar compounds.

4. Conclusions

Simultaneous destruction of toluene and naphthalene as tar surrogate has been investigated via steam reforming in a gliding arc discharge plasma. The addition of 4% steam into the plasma system significantly increased both the conversions of toluene and naphthalene, as the generated ·OH radicals are highly active in the oxidation of toluene and naphthalene and their fragments. H_2, C_2H_2 and CO, are the major gaseous products produced in the process, upgrading the producer gas simultaneously with tar destruction.

Toluene and naphthalene conversions reached 85.9% and 68.9%, respectively, at a tar concentration of 2 g/Nm^3, but were both decreased remarkably when further rising the tar concentration. The addition of CO_2 decreased both the tar conversions and energy efficiency due to the reduced density of N_2 excited species in the system. With rising preheating temperature, the tar conversions firstly increased but then slightly dropped. The formation of gaseous products is strongly dependent on the concentration of steam or CO_2 but almost independent of the preheating temperature.

Optical emission spectroscopic diagnostics demonstrated the formation of CN, ·OH, H·, NH and NO in the plasma steam reforming of mixed toluene and naphthalene. Various monocyclic and bicyclic aromatic compounds are the major liquid byproducts formed in this process. Energetic electrons, N_2 excited species, ·OH radicals (in the presence of H_2O) and O (in the presence of CO_2 or H_2O, with minor role) can all contribute to the initial destruction of toluene and naphthalene, producing benzyl, phenyl, cyclopentadiene, naphthyl and indenyl, etc. for the subsequent complex reactions.

Because of the complexity of the tar component, the performance of tar destruction by using non-

thermal plasmas in a practical gasifier will be significantly lowered compared to the destruction process of individual tar compound in laboratory researches. Therefore, further studies are still highly needed for the optimization of this technology.

Acknowledgments

The support of work by the National Natural Science Foundation of China (No. 51576174, No. 51706204), the Science Fund for Creative Research Groups of the National Natural Science Foundation of China (No. 51621005)) and the China Postdoctoral Science Foundation (No. 2018M630673) is gratefully acknowledged. Xin Tu acknowledges the EPSRC SUPERGEN Bioenergy Challenge (Ref. EP/M013162/1), EPSRC Impact Acceleration Account (IAA) and the European Union (EU) and Horizon 2020 funding awarded under the Marie Sklodowska-Curie action to the EUROPAH consortium (No. 722346). Fengsen Zhu acknowledges the support of the UK-China Newton PhD Placement Project co-funded by British Council (UK) and China Scholarship Council (CSC).

Declarations of interest: none

References

[1] S. Liu, D. Mei, L. Wang, X. Tu, Steam reforming of toluene as biomass tar model compound in a gliding arc discharge reactor, Chem. Eng. J. 307 (2017) 793-802.

[2] A. Bogush, J. Stegemann, A. Roy, Changes in composition and lead speciation due to water washing of air pollution control residue from municipal waste incineration, J. Hazard. Mater. 361 (2019) 187-199.

[3] K. Tao, N. Ohta, G. Liu, Y. Yoneyama, T. Wang, N. Tsubaki, Plasma enhanced catalytic reforming of biomass tar model compound to syngas, Fuel 104 (2013) 53-57.

[4] T. Nunnally, A. Tsangaris, A. Rabinovich, G. Nirenberg, I. Chernets, A. Fridman, Gliding arc plasma oxidative steam reforming of a simulated syngas containing naphthalene and toluene, Int. J. Hydrogen Energ. 39 (2014) 11976-11989.

[5] P. Jamróz, W. Kordylewski, M. Wnukowski, Microwave plasma application in decomposition and steam reforming of model tar compounds, Fuel Process Technol. 169 (2018) 1-14.

[6] F. Saleem, K. Zhang, A. Harvey, Role of CO_2 in the Conversion of toluene as a tar surrogate in a nonthermal plasma dielectric barrier discharge reactor, Energ. Fuel 32 (2018) 5164-5170.

[7] L. Liu, Q. Wang, S. Ahmad, X. Yang, M. Ji, Y. Sun, Steam reforming of toluene as model biomass tar to H_2-rich syngas in a DBD plasma-catalytic system, J. Energy Inst. 91 (2018) 927-939.

[8] H. Medeiros, A. Pilatau, O. Nozhenko, A. da Silva Sobrinho, G. Petraconi Filho, Microwave air plasma applied to naphthalene thermal conversion, Energ. Fuel 30 (2016) 1510-1516.

[9] L. Brusetti, S. Ciccazzo, L. Borruso, M. Bellucci, C. Zaccone, L. Beneduce, Metataxonomy and functionality of wood-tar degrading microbial consortia, J. Hazard. Mater. 353 (2018) 108-117.

[10] G. Guan, M. Kaewpanha, X. Hao, A. Abudula, Catalytic steam reforming of biomass tar: prospects and challenges, Renew. Sust. Energ. Rev. 58 (2016) 450-461.

[11] V.A. Bityurin, E.A. Filimonova, G.V. Naidis, Simulation of naphthalene conversion in biogas initiated by pulsed corona discharges, IEEE T. Plasma Sci. 37 (2009) 911-919.

[12] S. Anis, Z. Zainal, Tar reduction in biomass producer gas via mechanical, catalytic and thermal methods: A review, Renew. Sust. Energ. Rev. 15 (2011) 2355-2377.

[13] S. Zhang, M. Asadullah, L. Dong, H.-L. Tay, C.-Z. Li, An advanced biomass gasification technology with integrated catalytic hot gas cleaning. Part II: Tar reforming using char as a catalyst or as a catalyst support, Fuel 112 (2013) 646-653.

[14] A. Fridman. Plasma chemistry. Cambridge University Press, New York, 2008.

[15] H. Zhang, X. Li, F. Zhu, K. Cen, C. Du, X. Tu, Plasma assisted dry reforming of methanol for clean syngas production and high-efficiency CO_2 conversion, Chem. Eng. J. 310 (2017) 114-119.

[16] R. Snoeckx, A. Ozkan, F. Reniers, A. Bogaerts, The quest for value- added products from carbon dioxide and water in a dielectric barrier discharge: A Chemical Kinetics Study. ChemSusChem 10 (2017) 409-424.

[17] L. Liu, Q. Wang, J. Song, S. Ahmad, X. Yang, Y. Sun, Plasma-assisted catalytic reforming of toluene to hydrogen rich syngas, Catal. Sci. Technol. 7 (2017) 4216-4231.

[18] N. Tippayawong, P. Inthasan, Investigation of light tar cracking in a gliding arc plasma system, Int. J. Chem. React. Eng. 8 (2010): articleA50.

[19] Y.C. Yang, Y.N. Chun, Naphthalene destruction performance from tar model compound using a

gliding arc plasma reformer, Korean J. Chem. Eng. 28 (2011) 539-543.

[20] H.L. Chen, H.M. Lee, S.H. Chen, Y. Chao, M.B. Chang, Review of plasma catalysis on hydrocarbon reforming for hydrogen production—interaction, integration, and prospects, Appl. Catal. B-Environ. 85 (2008) 1-9.

[21] A. Fridman, S. Nester, L.A. Kennedy, A. Saveliev, O. Mutaf-Yardimci, Gliding arc gas discharge, Prog. Energ. Combust. Sci. 25 (1999) 211-231.

[22] H. Zhang, W. Wang, X. Li, L. Han, M. Yan, Y. Zhong, X. Tu, Plasma activation of methane for hydrogen production in a N_2 rotating gliding arc warm plasma: A chemical kinetics study, Chem. Eng. J. 345 (2018) 67-78.

[23] F. Zhu, X. Li, H. Zhang, A. Wu, J. Yan, M. Ni, H. Zhang, A. Buekens, Destruction of toluene by rotating gliding arc discharge, Fuel 176 (2016) 78-85.

[24] Y. Guo, X. Liao, J. He, W. Ou, D. Ye, Effect of manganese oxide catalyst on the dielectric barrier discharge decomposition of toluene, Catal. Today 153 (2010) 176-183.

[25] M. Ondarts, W. Hajji, J. Outin, T. Bejat, E. Gonze, Non-Thermal Plasma for indoor air treatment: Toluene degradation in a corona discharge at ppbv levels, Chem. Eng. Res. Des. 118 (2017) 194-205.

[26] H. Zhang, F. Zhu, X. Li, K. Cen, C. Du, X. Tu, Rotating gliding arc assisted water splitting in atmospheric nitrogen, Plasma Chem. Plasma P. 36 (2016) 813-834.

[27] N. Blin-Simiand, F. Jorand, L. Magne, S. Pasquiers, C. Postel, J.-R. Vacher, Plasma reactivity and plasma-surface interactions during treatment of toluene by a dielectric barrier discharge, Plasma Chem. Plasma P. 28 (2008) 429-466.

[28] J. Gao, J. Zhu, A. Ehn, M. Aldén, Z. Li, In-Situ Non-intrusive Diagnostics of Toluene Removal by a Gliding Arc Discharge Using Planar Laser-Induced Fluorescence, Plasma Chem. Plasma P. 37 (2017) 433-450.

[29] Z. Ye, S.K. Veerapandian, I. Onyshchenko, A. Nikiforov, N. De Geyter, J.-M. Giraudon, J.-F. Lamonier, R. Morent, An in-Depth Investigation of Toluene Decomposition with a Glass Beads-Packed Bed Dielectric Barrier Discharge Reactor, Ind. Eng. Chem. Res. 56 (2017) 10215-10226.

[30] A. Jess, Mechanisms and kinetics of thermal reactions of aromatic hydrocarbons from pyrolysis of solid fuels, Fuel 75 (1996) 1441-1448.

[31] A. Trushkin, I. Kochetov, Simulation of toluene decomposition in a pulse-periodic discharge operating in a mixture of molecular nitrogen and oxygen, Plasma Phys. Rep+ 38 (2012) 407-431.

[32] R.M. Eliott, M.F. Nogueira, A.S. Silva Sobrinho, B.A. Couto, H.S. Maciel, P.T. Lacava, Tar reforming under a microwave plasma torch, Energ. Fuel 27 (2013) 1174-1181.

[33] L. Yu, X. Li, X. Tu, Y. Wang, S. Lu, J. Yan, Decomposition of naphthalene by dc gliding arc gas discharge, J. Phys. Chem. C 114 (2009) 360-368.

[34] Y.N. Chun, S.C. Kim, K. Yoshikawa, Destruction of anthracene using a gliding arc plasma reformer, Korean J. Chem. Eng. 28 (2011) 1713.

[35] H. Zhang, F. Zhu, X. Li, K. Cen, C. Du, X. Tu, Enhanced hydrogen production by methanol decomposition using a novel rotating gliding arc discharge plasma, RSC Adv. 6 (2016) 12770-12781.

[36] P. Parthasarathy, K.S. Narayanan, Hydrogen production from steam gasification of biomass: Influence of process parameters on hydrogen yield–A review, Renew. Energ. 66 (2014) 570-579.

[37] National Institute of Standards and Technology. NIST Chemical Kinetics Database, https://kinetics.nist.gov/kinetics/index.jsp; 2015 [accessed 10 August 2018].

[38] M. Hübner, R. Brandenburg, Y. Neubauer, J. Röpcke, On the Reduction of Gas- Phase Naphthalene Using Char–Particles in a Packed–Bed Atmospheric Pressure Plasma, Contrib. Plasm Phys. 55 (2015) 747-752.

[39] H. Huang, D. Ye, D.Y. Leung, F. Feng, X. Guan, Byproducts and pathways of toluene destruction via plasma-catalysis, J. Mol. Catal. A-Chem. 336 (2011) 87-93.